ORIGINAL PAPER

Summertime variability of Mediterranean evaporation: competing impacts from the mid latitudes teleconnections and the South Asian monsoon

Igor I. Zveryaev[1] · Abdel A. Hannachi[2]

Abstract

Interannual variability of Mediterranean evaporation and its links to regional climate during summer are investigated based on evaporation data from the Woods Hole Oceanographic Institution dataset. An EOF (Empirical Orthogonal Function) analysis performed on the monthly means (i.e., separately for June, July, August, and September time series) revealed two leading modes of evaporation variability, characterized by the monopole (EOF-1) and zonal dipole (EOF-2) patterns. These modes explain altogether more than 60% of the total variability of Mediterranean evaporation for each month. In all summer months, the EOF-1 reflects an interdecadal change signal characterized by below normal evaporation in 1970–2000 and above normal evaporation before and after this period. This mode is associated with the Atlantic Multidecadal Oscillation. The EOF-2 pattern reflects interannual variations of Mediterranean evaporation that differ significantly from month to month. The reason for this difference is the changing roles of regional teleconnections, such as the summer North Atlantic Oscillation (SNAO), the Scandinavian and East Atlantic teleconnections, and the Asian monsoon. The impacts of these teleconnections on Mediterranean evaporation are highly variable both in space and time. The largest impact of the SNAO on Mediterranean evaporation is detected in early summer, but its impact weakens and disappears towards the end of the summer season. An opposite tendency is obtained with the Asian monsoon, having the strongest impact on evaporation in late summer. The study suggests that these teleconnections impact Mediterranean evaporation mostly through atmospheric dynamics (the SNAO) and thermodynamics (the Asian monsoon) in early and late summer respectively.

1 Introduction

Climate of the Mediterranean region varies significantly on a wide range of time scales (e.g., Lionello 2012). This is also true for the regional hydrological cycle. It was particularly found that during recent decades Mediterranean evaporation increased, whereas regional precipitation decreased (e.g., Mariotti 2010; Allan and Zveryaev 2011), resulting in significant increase in the loss of fresh water from the Mediterranean Sea into the atmosphere, accompanied with

increasing surface salinity. Model simulations also imply further acceleration of the increase in fresh water deficit in the current century (e.g., Mariotti et al. 2008), calling for further investigation of the consequences. A deeper understanding of the regional hydrological cycle and its variability and changes at different time scales could lead to a better adaptation and mitigation strategy for the Mediterranean region. Equally important is the effect on surface salinity and sea surface temperature, which can affect the deep water formation as well as the inflow-outflow through Gibraltar Strait, with implication on long-term changes in the water balance in the basin (Borghini et al. 2014), in addition to the ecological and socio-economical impact (Sandoval-Gil et al. 2012).

Evaporation is the largest term in the Mediterranean fresh water budget, whereas annual precipitation is only about half the evaporation (Mariotti et al. 2002). Thus, the understanding of interannual variability of Mediterranean evaporation is crucial for an objective assessment of changes in the regional hydrological cycle and surface salinity and temperature. It is

---

✉ Abdel A. Hannachi
   a.hannachi@misu.su.se

[1] P.P. Shirshov Institute of Oceanology, Russian Academy of Sciences, Moscow, Russia

[2] Department of Meteorology, MISU, Stockholm University, Stockholm, Sweden

now well understood (see e.g., Zveryaev and Hannachi 2012, 2017; Papadopoulos et al. 2012) that during the cold season interannual variability of Mediterranean evaporation is driven mostly by the East Atlantic (EA) and East Atlantic—West Russia (EAWR) teleconnections (Barnston and Livezey 1987). However, in summer, when atmospheric circulation anomalies in mid latitudes are weaker and less pronounced, compared to winter, the general picture of the mechanisms driving interannual variability of Mediterranean evaporation is not so clear and not well understood. There are indications of the impact of the Atlantic Multidecadal Oscillation (AMO, e.g., Enfield et al. 2001) on Mediterranean climate in general and evaporation in particular (e.g., Zveryaev and Hannachi 2012; O'Reilly et al. 2017). This impact is best pronounced during the summer season. A few studies (e.g., Simpson et al. 2015) suggest an important role of Middle East topography in variability of regional evaporation during the summer season. Recent studies suggest that the summer climate of Eastern Mediterranean is impacted by the summer North Atlantic Oscillation (SNAO, e.g., Chronis et al. 2011) and by the South Asian monsoon through teleconnection and stationary Rossby waves (e.g., Hoskins and Ambrizzi 1993). The effect of the summer Asian monsoon on the Mediterranean has been discussed in a number of studies (e.g., Cherchi et al. 2014; Fontaine et al. 2011; Rizou et al. 2015). The Indian summer monsoon convection triggers propagating Rossby wave reaching the Eastern Mediterranean and forces subsidence within a high pressure system, which can enhance surface northerlies. The latter acts through the so-called monsoon-desert mechanism (Rodwell and Hoskins 1996). It should be stressed, however, that many of the above studies analyzing regional key climate variables (e.g., precipitation, air temperature, sea surface temperature), do not consider summertime Mediterranean evaporation, which needs further investigation to enhance our understanding. Thus, the main focus of the present study is the structure of Mediterranean evaporation variability on interannual time scales during the summer season. Besides the structure of summer evaporation variability, we hope to get deeper insight into the mechanisms driving this variability.

The present study analyzes interannual variability of Mediterranean evaporation during extended summer season (June–September, JJAS) using gridded evaporation data (Yu and Weller 2007; Yu 2007). We also explore some of the basic mechanisms driving Mediterranean evaporation variability by examining links between the leading modes of Mediterranean evaporation and some key regional climate variables. The data used and analysis methods are described in "section 2." "Section 3" analyses the spatial-temporal structure of the leading modes of the summer monthly mean evaporation for 1958–2015. "Section 4" examines the links of the summertime Mediterranean evaporation to regional atmospheric teleconnections, as well as to key climate variables

impacting evaporation, thus, revealing the major driving mechanisms. A summary and discussion are presented in the last section.

2 Data and methods

In the present analysis, we used evaporation data from the Woods Hole Oceanographic Institution (WHOI) OAFlux data set (Yu and Weller 2007). This data set is obtained by objectively blending satellite data with numerical weather prediction (NWP) model outputs while using in situ observations to determine the weights used in the assimilation process (Yu and Weller 2007). The OAFlux data set provides evaporation (and other variables) data on a $1° \times 1°$ latitude-longitude grid over the global oceans for 1958–2015. In addition, we also used near surface specific humidity and wind speed from this dataset. Detailed description of the data and the synthesis procedure can be found in Yu and Weller (2007) and at the institution website[1].

To investigate the links between variability of the Mediterranean evaporation and regional atmospheric circulation, we used indices of the major teleconnection patterns that have been documented and described by Barnston and Livezey (1987). The patterns and indices were obtained by applying rotated principal component analysis (e.g., Hannachi et al. 2007; Hannachi 2021) to standardized 500 hPa height anomalies in the Northern Hemisphere. The teleconnection patterns used here to examine links to Mediterranean evaporation include, in addition to the SNAO, the East Atlantic (EA), East Atlantic—West Russia (EAWR) and the Scandinavian (SCA) patterns. These regularly updated indices, covering the period 1950—present, are available from the Climate Prediction Centre (CPC) website.[2] Further details on the teleconnection pattern calculation procedures can be found in Barnston and Livezey (1987) and at the CPC website. To explore the links between Mediterranean evaporation and South Asian monsoon, we used well-known monsoon indices, namely, the Webster and Yang index (WYI) and all India rainfall index, AIRI (Webster and Yang 1992; Parthasarathy et al. 1995) characterizing monsoon dynamics.

To explore the spatial-temporal structure of interannual variability of the monthly summer Mediterranean evaporation, we apply empirical orthogonal function (EOF) analysis using the covariance matrix of the Mediterranean evaporation anomalies (Wilks 1995; von Storch and Navarra 1995; Hannachi et al. 2007). These anomalies are obtained by subtracting the mean annual cycle from the original evaporation data at each grid point. The anomalies are then de-trended by removing the long-term linear trend. To take into account

---

[1] http://oaflux.whoi.edu.

[2] http://www.cpc.ncep.noaa.gov/data/teledoc/telecontents.html.

the latitudinal distortions, the obtained (de-trended) anomalies were area-weighted using the square root of the cosine of latitude (North et al. 1982). The EOF method is a classical exploratory tool, which has some weakenesses, including mixing (e.g., Hannachi 2021), but is a convenient exploratory tool particularly for moderate sample sizes.

Conventional correlation analysis has been applied to study the links to teleconnection patterns and the key climate variables complemented with a multiple regression analysis. In this study, we consider only simultaneous connections between the summer Mediterranean evaporation and major teleconnection patterns and the climate variables. According to the Student's t-test (Bendat and Piersol 1966), the minimum significant correlation coefficients between the time series analyzed are 0.26 for the 5% significance level.

3 Leading modes of Mediterranean evaporation during summer

To investigate the spatial-temporal structure of interannual variability of Mediterranean evaporation during summer and explore its seasonal (i.e., month-to-month) evolution, we performed an EOF analysis of the monthly mean evaporation anomalies separately for June, July, August, and September for the period 1958–2015. Given that the leading two EOF modes, in each month, explain about or more than 60% of total variability (Table 1), we have limited our analysis to these modes. We note, in particular, that the leading EOF is well separated from the remaining EOFs. The spatial patterns of the leading two EOFs and associated principal components (PCs) for each summer month are shown in Figs. 1–4.

The first EOF explains from about 44% (in September) to 48% (in July) of the total variance of the Mediterranean evaporation (Table 1). In all summer months, the spatial pattern of EOF-1 (Fig. 1) reflects coherent variations of evaporation over the entire Mediterranean basin. It is worth noting, however, that in different months the largest loadings are observed in different parts of the Mediterranean Sea. Obviously, the patterns in July (Fig. 1b) and August (Fig. 1c) are similar, with the largest loadings in the western part of the basin, but in June (Fig. 1a) and September (Fig. 1d) the respective EOF-1 patterns are different implying that associated variability of evaporation might be impacted by different mechanisms. For all summer months, the respective PCs of EOF-1 (Fig. 2) reveal a clear interdecadal signal with prevailing below normal evaporation from the early 1970s to the late 1990s, and above normal evaporation before and after that period. Similarity of temporal behavior of the first PCs is complemented by relatively large correlations between respective time series (Table 2). These results are generally consistent with previous analyses of seasonal mean global and Mediterranean evaporation (e.g., Yu, 2007; Zveryaev and Hannachi 2012) which show large interdecadal signal in summer evaporation.

Contribution of the second EOF to the total Mediterranean evaporation variance varies from around 14% (in June) to about 22% (in September). The spatial patterns of this mode of variability are characterized by a zonal dipole (Fig. 3) with opposite variations of evaporation in the eastern and western parts of the Mediterranean Sea. Note, in particular, the largest loadings in both centers revealed in September (Fig. 3d), recalling that this EOF-2 explains the largest (compared to other months) fraction of the total evaporation variance (Table 1). Despite the obvious similarity between the spatial patterns, the associated PCs (Fig. 4) show quite different interannual variability during different summer months, which is corroborated by the low and insignificant correlations between respective time series (Table 2).

To summarize results of this section, we note that the major differences for EOF-1 of Mediterranean evaporation are observed in location of the largest loadings, whereas the temporal behavior of the leading PC is similar and shows a clear interdecadal signal with negative evaporation anomalies in the period from the early 1970s to the late 1990s and positive anomalies before and after that period. For the EOF-2, the associated PCs show shorter-term interannual variability, which, in contrast to EOF-1, differs significantly with different summer months (Fig. 4), thus, implying different driving mechanisms of Mediterranean evaporation variability. To explore these mechanisms impacting Mediterranean evaporation variability during summer, we examine in the next section the links between the leading EOFs of evaporation and known regional climate signals that potentially might play a role.

4 Relation to the regional climate

4.1 Links to regional atmospheric teleconnections

To investigate the links between summertime variability of Mediterranean evaporation and regional atmospheric circulation, we first compute correlations (Table 3) between the leading PCs of evaporation and indices of regional teleconnections (Barnston and Livezey 1987) as well as indices of the Asian summer monsoon (Webster and Yang 1992; Parthasarathy et al. 1995).

Table 1 Fractions (in %) of the total Mediterranean evaporation variability explained by the leading EOFs

|	June	July	August	September
EOF-1	45.98	48.19	44.10	43.93
EOF-2	13.91	19.90	17.01	21.97
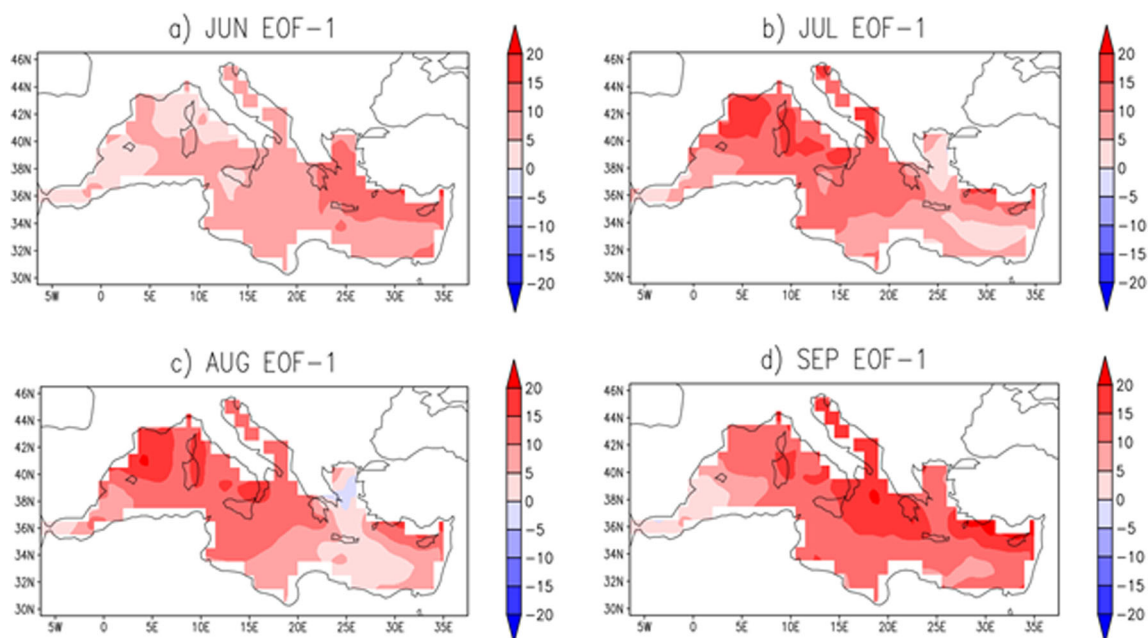
Fig. 1 Spatial patterns of the EOF-1 mode of the summer monthly mean evaporation (1958–2015)

In general, the obtained correlations show rather moderate, but statistically significant, relations with the Asian monsoon (in September), SNAO (in June), SCA, EAWR, and AMO. Note that these relations vary significantly during the summer season (Table 3). For a given month, Mediterranean evaporation might be impacted simultaneously by the different climate signals, like in August and September (see Table 3), which can potentially offset (or mask) each other. Furthermore, different signals may impact evaporation in different parts of the Mediterranean basin.

Thus, when we consider the leading EOFs describing basin-scale evaporation variability, we get relatively low correlations with regional teleconnections. Therefore, to assess the spatial structure of the relationships between teleconnections and Mediterranean evaporation, we further investigate direct correlations between teleconnection indices and evaporation at each grid point (Figs. 5 and 6).

Since previous studies suggest an impact of both the Asian monsoon (e.g., Cherchi et al. 2014; Rizou et al. 2015) and the
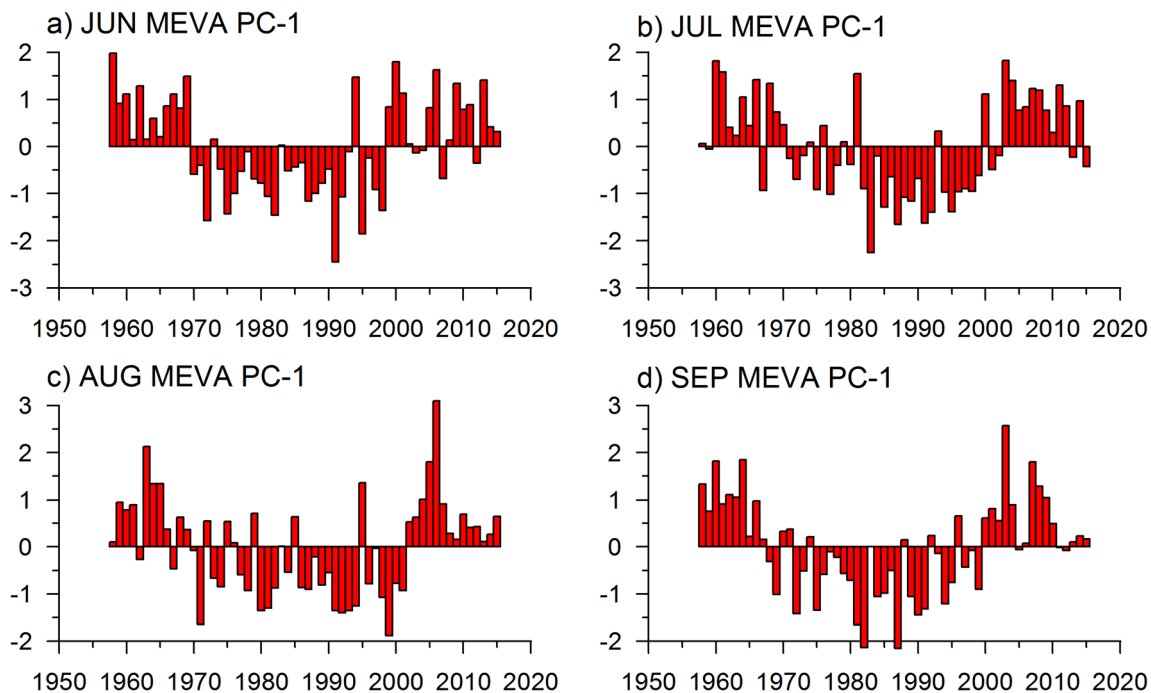
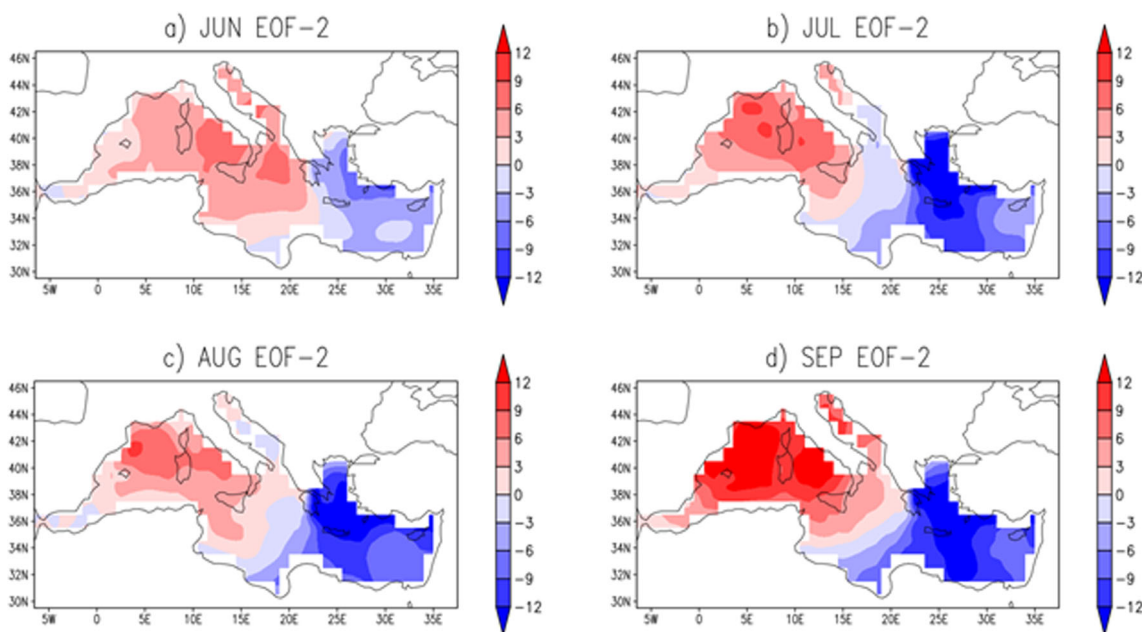Fig. 2 Principal components of the EOF-1 mode of the summer monthly mean evaporation

Fig. 3 Spatial patterns of the EOF-2 mode of the summer monthly mean evaporation (1958–2015)

SNAO (e.g., Chronis et al. 2011) on Mediterranean summer climate, particularly in the eastern part, we first examine links of the Asian monsoon indices (WYI and AIRI) and the SNAO index, with Mediterranean evaporation in each summer month. It should be stressed that to our knowledge none of the above studies considered influence of the monsoon (and the SNAO) on Mediterranean evaporation. As seen from Fig. 5, the strongest links between Mediterranean evaporation, especially in the eastern part, and WYI and AIRI indices are revealed in September

(Fig. 5j, k), i.e., during the mature phase of monsoon. The correlation pattern for WYI shows stronger links, compared to that for AIRI, which can possibly be explained by the discontinuous nature of rainfall, compared to the continuous WY index. The pattern generally suggests that strong Asian monsoon results in enhanced (reduced) evaporation in the eastern (western) part of the Mediterranean basin (Fig. 5j). In contrast to the Asian monsoon, the largest impact from the SNAO is found in early summer (e.g., June, Fig. 5c). In June, the correlation pattern for the
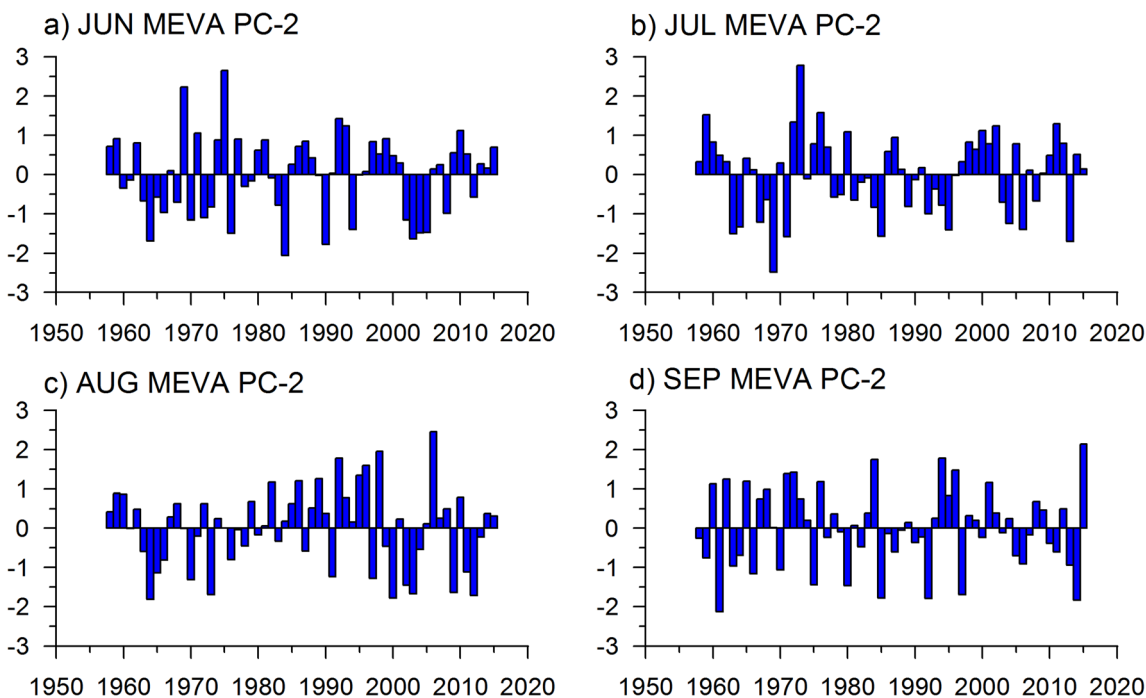

Fig. 4 Principal components of the EOF-2 mode of the summer monthly mean evaporation

Table 2 Correlations between leading PCs of Mediterranean evaporation variability during the summer season. Significant correlations at 5% level are highlighted

	Jun/Jul	Jun/Aug	Jun/Sep	Jul/Aug	Jul/Sep	Aug/Sep
PC-1	**0.45**	**0.26**	**0.48**	**0.43**	**0.56**	**0.38**
PC-2	− 0.05	**0.29**	− 0.25	− 0.24	0.03	0.04

SNAO reveals a well pronounced zonal dipole with significant negative (positive) correlations in northwestern (southeastern) parts of the basin (Fig. 5c). Significant negative correlations are also obtained in the western part of the basin in July (Fig. 5f). However, in late summer (i.e., August, September), the impact of the SNAO vanishes (Fig. 5i, l). In summary, the results generally demonstrate strengthening (weakening) of the Asian monsoon (the SNAO) impact on Mediterranean evaporation towards the end of the summer season.

We have also examined the relationship between the other regional teleconnections and summertime Mediterranean evaporation variability. Correlation patterns for the SCA, EA, and EAWR teleconnections are shown in Fig. 6. The largest correlations of Mediterranean evaporation with the SCA and EA indices are found in August (Fig. 6 g, h). Significant links with SCA are detected over most of the Mediterranean basin (Fig. 6 g), and suggest that the positive (negative) phase of the SCA is associated with enhanced (reduced) Mediterranean evaporation. Significant negative correlations with the EA over the central and eastern Mediterranean (Fig. 6 h) imply that during positive (negative) phase of EA evaporation in these sub-basins is reduced (enhanced). Similar relationships between the EAWR teleconnection and evaporation in the western part of the Mediterranean Sea are found in September (Fig. 6 l). Thus, altogether the results of this sub-section demonstrate highly variable (both in space and time) impacts of the Asian monsoon and regional teleconnections on variability of Mediterranean evaporation during the summer season.

Table 3 Correlations between leading PCs of Mediterranean evaporation variability and indices of regional teleconnections

	June		July		August		September	
	PC-1	PC-2	PC-1	PC-2	PC-1	PC-2	PC-1	PC-2
NAO		− 0.26						
SCA				0.39	0.33			
EA								− 0.35
AMO					0.32	0.31		
WY							0.38	
IMI							0.36	

4.2 Relative roles of atmospheric dynamics and thermodynamics in teleconnection impacts on summer Mediterranean evaporation

The near surface wind speed (ws) and the near surface specific humidity (qa) are respectively major dynamic and thermodynamic drivers of evaporation variability. Thus, to reveal which of these drivers is more important in controlling teleconnection impacts on Mediterranean evaporation, we further examine links between these variables and the teleconnections. Correlations between near surface wind speed ws and specific humidity qa on one side and the (September) WYI and (June) SNAO time series on the other are depicted in Fig. 7. Note, for the sake of completeness, we also repeat here respective correlation patterns for evaporation.

The correlation patterns for the WY index clearly suggest a thermodynamic impact of the Asian monsoon on Mediterranean evaporation in September (Fig. 7a, c). Specifically, strong (weak) monsoon is associated with reduced (enhanced) qa in eastern Mediterranean and enhanced (reduced) qa in northwestern Mediterranean Sea (Fig. 7c). This results in opposite changes of the vertical moisture gradient leading to enhanced (reduced) evaporation in eastern Mediterranean during strong (weak) monsoon, and opposite tendencies in northwestern Mediterranean Sea (Fig. 7a). There is also an indication of dynamic impact of the Asian monsoon on Mediterranean evaporation, i.e., through enhanced ws in eastern Mediterranean during the strong monsoon (Fig. 7e). The figure suggests, nevertheless, that the thermodynamic impact of the Asian monsoon on Mediterranean evaporation is dominant.

Similarly, we examine the roles of atmospheric dynamics and thermodynamics in the SNAO impact on Mediterranean evaporation in June. In contrast to the Asian monsoon, the thermodynamic impact of the SNAO on Mediterranean evaporation is very weak and highly localized (e.g., over the Aegean Sea and over the southern part of central Mediterranean, Fig. 7d). The SNAO mostly impacts Mediterranean evaporation through changes in regional atmospheric dynamics (i.e., changes in near surface ws, Fig. 7f). This generally means that strong (weak) wind induces enhanced (reduced) evaporation in particular region. This kind of impact is best pronounced over the northern and easternmost parts of the basin (Fig. 7f). This is consistent with the result of Kostopuolou and Jones (2007) who found a main center of action of the summer sea level pressure over eastern Mediterranean. They also found, based on daily data, that during summer the main centers of action affecting climate conditions over eastern Mediterranean are mostly related to the North Atlantic anticyclone and the summer Asian thermal low. Thus, although the correlation patterns for evaporation (Fig. 7a, b) are comparable, we find different mechanisms of the Asian monsoon and the SNAO impacts on Mediterranean evaporation.
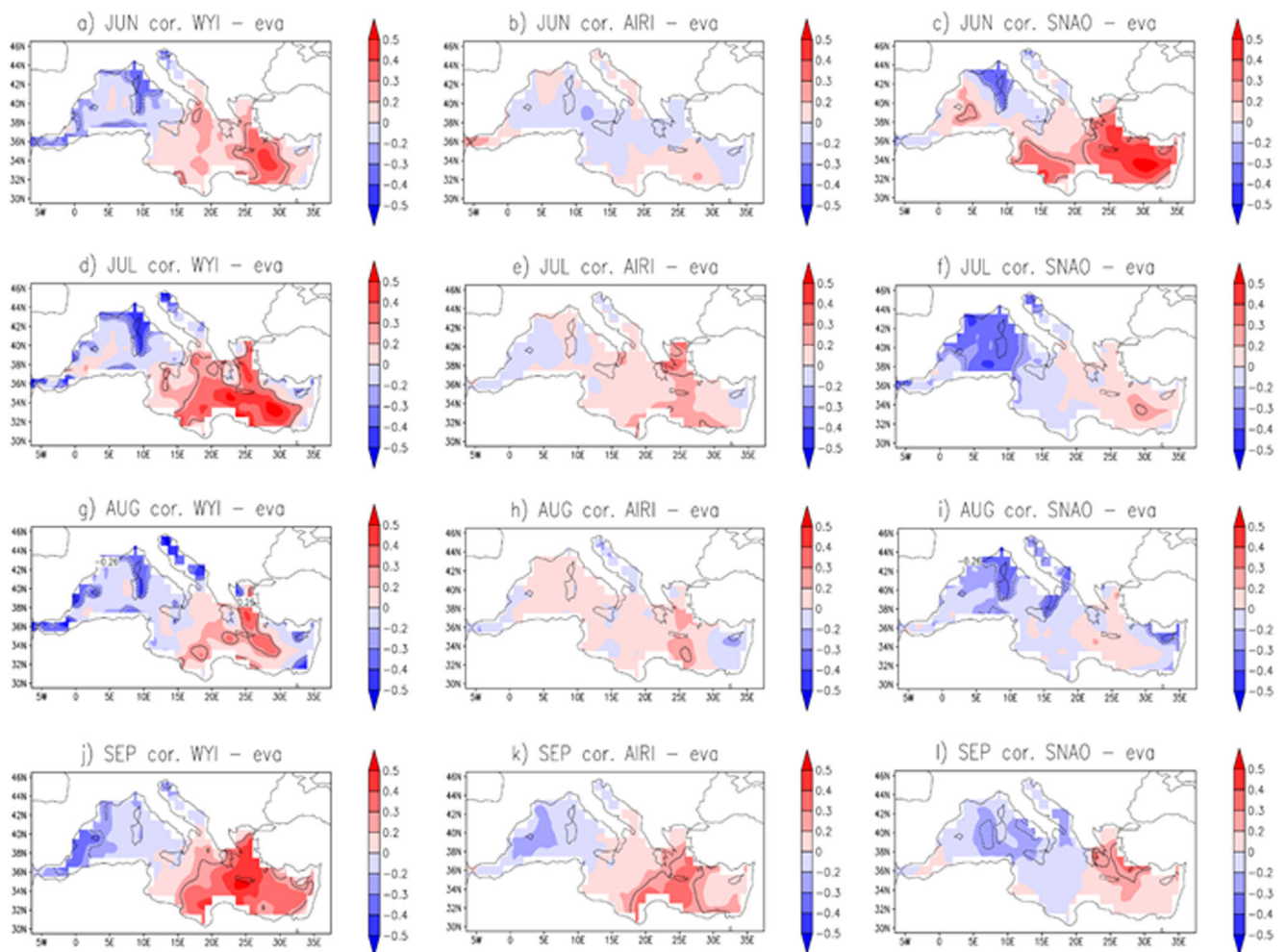
Fig. 5 Correlations between Mediterranean evaporation and WYI index (**a**, **d**, **g**, **j**), AIRI index (**b**, **e**, **h**, **k**) and SNAO index (**c**, **f**, **i**, **l**). Black solid (dashed) curve indicates areas of significant positive (negative) correlations

Correlations of the SCA and EA teleconnections with evaporation, near surface specific humidity and wind speed in August are shown in Fig. 8. Correlation patterns for the SCA teleconnection generally imply that the basin-scale evaporation increase (decrease), see Fig. 8a, is caused by a decrease (increase) of q_a (Fig. 8c). While the thermodynamic mechanism is dominant, local dynamics (i.e., through the ws changes) impact from the SCA teleconnection is also clear (Fig. 8e). As we already noted, the positive (negative) phase of the EA teleconnection is associated with decreased (enhanced) evaporation (Fig. 8b). Again, this is mostly determined by thermodynamic processes (Fig. 8d). Specifically, during positive (negative) phase of the EA teleconnection q_a is enhanced (reduced) resulting in smaller (larger) vertical moisture gradient which leads to decreased (increased) evaporation (Fig. 8b). Note the EAWR impact on western Mediterranean evaporation in September (Fig. 6 l) is determined by atmospheric thermodynamics, though some influence of dynamics is also present (not shown).

To conclude, the analysis presented in this sub-section shows that in summer regional teleconnections impact Mediterranean evaporation both through atmospheric dynamics (near surface wind) and thermodynamics (near surface humidity). The relative roles of these two factors change significantly during the summer season. While atmospheric dynamics is a major player in early summer, as in the case of the SNAO impact in June, thermodynamics is mostly dominant in late summer, as in the case of the Asian monsoon impact in September. Thus, the mechanisms determining Mediterranean evaporation variability are principally different in early and late summer.

4.3 Multiple regression analysis

The undertaken analysis is based on simple correlations, which has no predictive power, though it has important exploratory research values. Furthermore, in the above correlation analysis, no specific timescale is highlighted that could
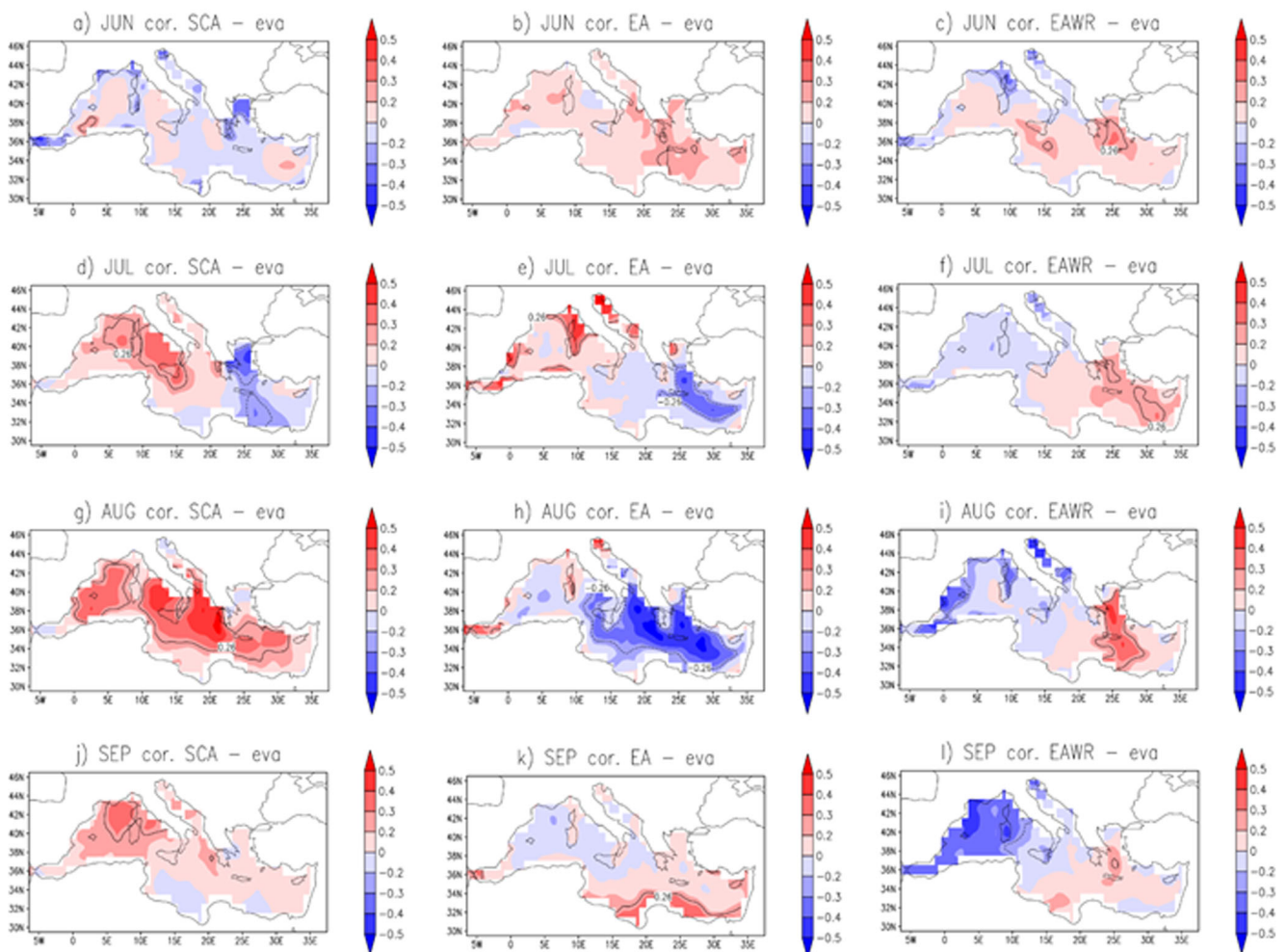
Fig. 6 Correlations between Mediterranean evaporation and SCA index (**a**, **d**, **g**, **j**), EA index (**b**, **e**, **h**, **k**) and EAWR index (**c**, **f**, **i**, **l**). Black solid (dashed) curve indicates areas of significant positive (negative) correlations

indicate more relevance to the basin evaporation. This can be done within a yet simple framework of multiple regression analysis using the evaporation PCs. Precisely, we investigate here the link between the leading modes of Mediterranean evaporation and five teleconnection indices in a unified framework using multiple linear regression model:

$$EvapPC = b1 \times NAO + b2 \times SCA + b3 \times EA + b4$$
$$\times EAWR + b5 \times WYI + error \qquad (1)$$

The analysis is performed using PC1 and PC2 of Mediterranean evaporation for the summer months, and we mainly focus, unless otherwise stated, on the 5% significance level. We recall here that the dominant timescales of PC1 and PC2, namely interdecadal and interannual respectively. The results are summarized in Table 4.

For June PC1, with its interdecadal fluctuation, the (summer) NAO is found to be the only significant predictor, although SCA also becomes significant at 10% level. For PC2, however, we find SNAO, EAWR and WYI are

significant predictors. In July, the R-square of the regression model of PC1 is very small and there is no significant link with all the teleconnections shown in model (1). For PC2, however, the R-square is 0.44 and EA and WYI are the only significant teleconnection predictors. This points to the effect of both EA and Asian summer monsoon in the mid-summer on interannual timescales. This supports the results of the previous section regarding EA, but not SCA and WYI, suggesting that particularly for WYI, which is dominated by interannual variability, the correlation analysis did not show significance, as the dominant timescale of the basin evaporation is multidecadal. In August, we found significant link to the SNAO, SCA, and EAWR for PC1 (R-square = 0.3) and only to the EA and EAWR for PC2. Finally, for September, none of the above teleconnections is linked significantly to PC1, although at 10% there is a link with EAWR. But for PC2, we obtain significant link with SNAO and WYI, with R-square value of 0.4. Note, in particular, the significant effect of the Asian monsoon mature phase on the Mediterranean evaporation, also in agreement with the previous section results, again
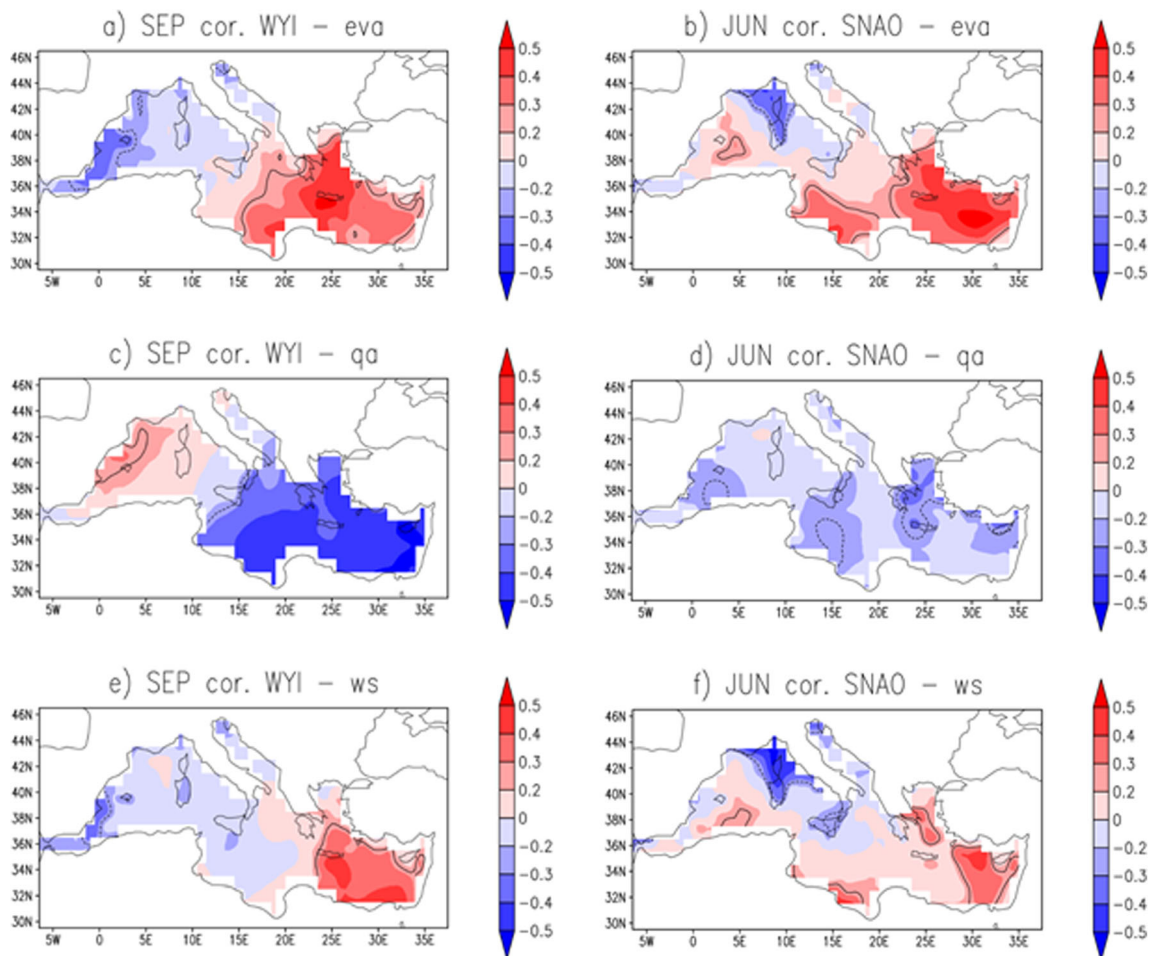
Fig. 7 Correlations between Mediterranean evaporation (**a**, **b**), near surface specific humidity (**c**, **d**), near surface wind speed (**e**, **f**) and WYI index (a, c, e) and SNAO index (b, d, f). Black solid (dashed) curve indicates areas of significant positive (negative) correlations

on interannual timescale. Interestingly, we find again an effect of the SNAO on Mediterranean evaporation in the range of interannual timescales.

It should be emphasized that the above analysis implies that only linear relationships are considered. Therefore, we complemented it by performing composites, which implies both linear and non-linear relationships between considered parameters. A composite analysis is conducted by computing, for a specific month, the difference of mean Mediterranean evaporation between cases with large (above +1 standard deviation) and small (below −1 standard deviation) SNAO and WYI. Basically, we obtained results similar to correlation analysis. Figure 9 shows the obtained composite for September evaporation reflecting its link to the Asian Monsoon (9a) and SNAO (9b). Although the small sample size does not allow for significance test, evidently, the obtained pattern is very similar to correlation patterns in Fig. 5 l (SNAO) and Fig 5j and k (WYI). Comparable results are obtained for the other months (not shown). Thus, the composite analysis confirms robustness of the results of correlation analysis discussed in the study, and suggests, based on the (rather small) available sample size, that

the mechanisms involved in Mediterranean evaporation-teleconnection link are dominated by linear or quasi-linear processes.

5 Summary and discussion

We explored the spatial-temporal structure of interannual variability of Mediterranean evaporation during extended (June–September) summer season based on the monthly data from the OAFlux data set (Yu and Weller 2007) for the period 1958–2015. We further investigated the links between the leading modes of Mediterranean evaporation and regional atmospheric teleconnections and Asian monsoon. Particular attention was paid to the seasonal (i.e., from June to September) evolution of these links. Finally, we explored the changing roles of atmospheric dynamics and thermodynamics in variability of Mediterranean evaporation during the summer season.

Two leading EOF modes, explaining altogether more than 60% of the summertime Mediterranean evaporation variability,
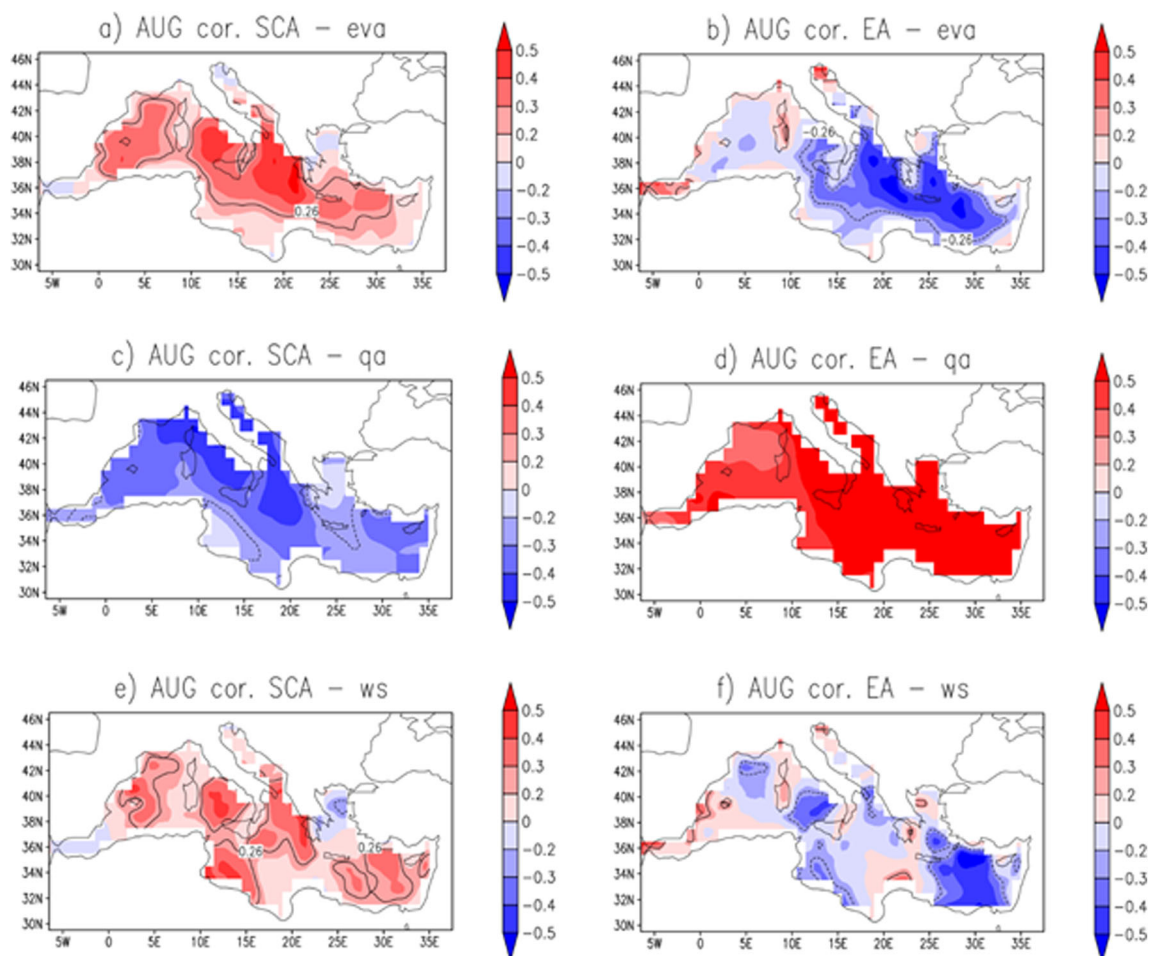
Fig. 8 Correlations between Mediterranean evaporation (**a**, **b**), near surface specific humidity (**c**, **d**), near surface wind speed (**e**, **f**) and SCA index (a, c, e) and EA index (b, d, f). Black solid (dashed) curve indicates areas of significant positive (negative) correlations

revealed similar spatial patterns (monopole for EOF-1 and zonal dipole for EOF-2) in all summer months. The principal components of EOF-1 are also similar in all months and reflect interdecadal changes of Mediterranean evaporation presumably associated with the AMO (e.g., Enfield et al. 2001). In contrast to EOF-1, the principal components of EOF-2 are different in different summer months and are associated with different climate signals (e.g., SNAO, SCA, Asian monsoon), thus, implying interannual changes of the major drivers of evaporation variability during summer. This suggests that the analysis of summer seasonal mean evaporation variability is not representative and cannot give an objective picture

Table 4 Regression coefficients from the regression model (1) along with the R-square and p values for PC1 and PC2 of Mediterranean evaporation for the extended summer months. Regression coefficients that are significant at 5% level are underlined

	b1	b2	b3	b4	b5	R-square	p-value
June PC1	− 0.31	0.26	− 0.19	− 0.12	− 0.04	0.19	0.02
PC2	0.30	0.03	− 0.01	0.24	0.43	0.43	0.
July PC1	0.2	− 0.13	− 0.13	0.04	− 0.04	0.09	0.28
PC2	− 0.15	0.17	0.26	− 0.10	− 0.38	0.44	0.
Aug PC1	0.24	− 0.31	0.09	0.21	0.15	0.29	0.
PC2	− 0.06	− 0.05	0.31	− 0.21	− 0.19	0.37	0.
Sep PC1	0.14	− 0.21	− 0.04	0.21	0.01	0.13	0.11
PC2	− 0.29	0.11	− 0.12	− 0.17	− 0.44	0.38	0.

Fig. 9 Composite of Mediterranean evaporation in September estimated as the difference between evaporation during strong and weak AIRI (a) and SNAO (b). Strong and weak are defined, respectively, as times when the index is greater then +1 std and less then − 1 std. Unit: cm
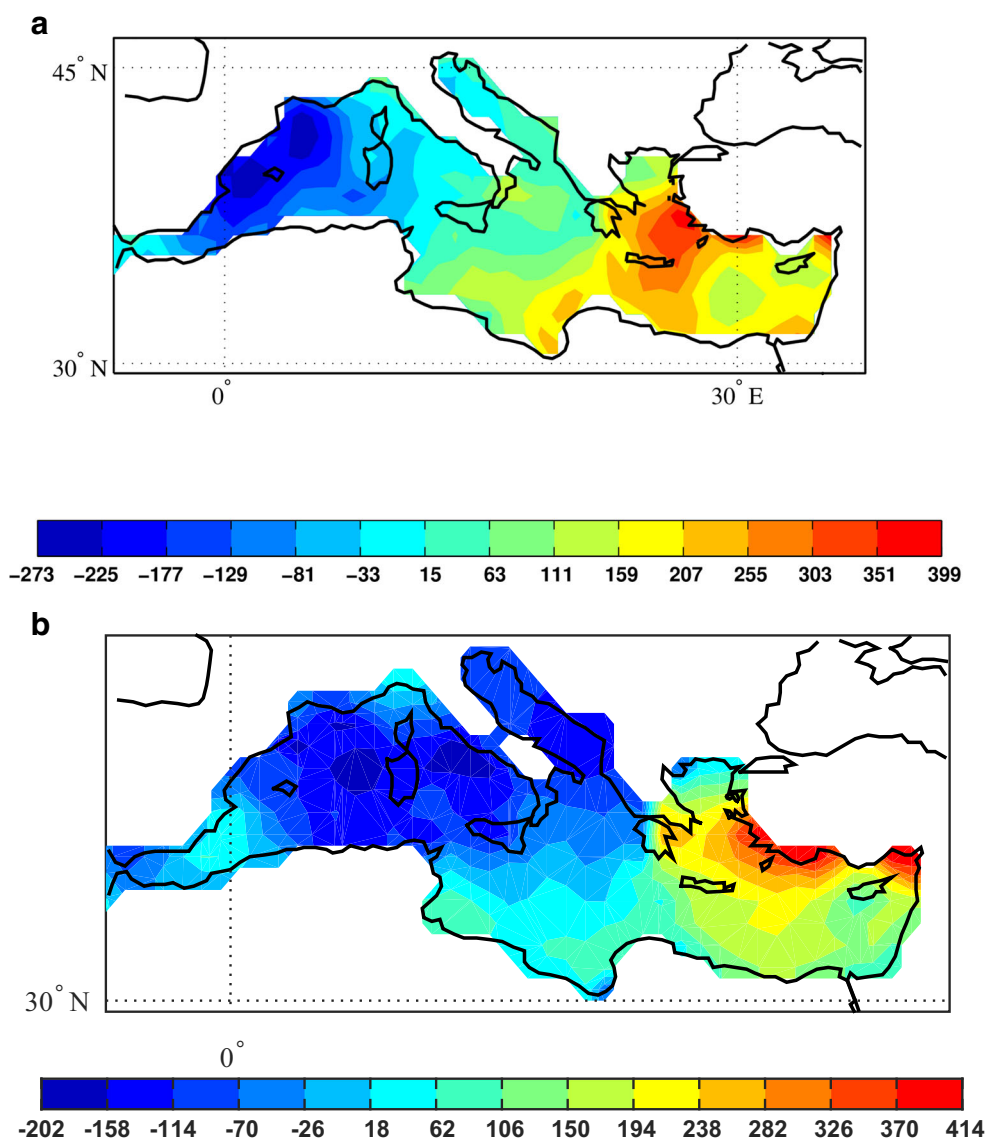
regarding its drivers. This is in striking contrast to winter when, during the entire season (i.e., in all winter months), variability of Mediterranean evaporation is driven by the EA and EAWR teleconnections which is reflected in analyses of both monthly and seasonal means (e.g., Papadopoulos et al. 2012; Zveryaev and Hannachi 2017).

Though our analysis revealed statistically significant links between the leading modes of Mediterranean evaporation and regional teleconnections, the obtained correlations are not large. Compared to winter, in summer season, the centers of action of pressure system (e.g., Icelandic low/Azores high) are not well developed, particularly in early summer. In addition, teleconnection patterns, such as SCA, EAWR, and even SNAO, may not be prominent (e.g., degenerate). These links can therefore be highly variable both in space and time. For example, we found strong impact of the Asian monsoon on Mediterranean evaporation in September (i.e.,

during mature phase of monsoon), but not in early summer, which can be explained by the variable monsoon onset dates (e.g., Soman and Kumar 1993; Pradhan et al. 2017). This result is broadly consistent with some previous studies (e.g., Rodwell and Hoskins 1996; Raicich et al. 2003; Cherchi et al. 2014), which, however, did not consider Mediterranean evaporation. Moreover, we show for the first time seasonal evolution of the monsoonal impact on Mediterranean evaporation.

In contrast to the Asian monsoon, the largest impact of the SNAO on Mediterranean evaporation is observed in early summer (i.e., June), and vanishes towards the end of the summer season. In some months, we also found large local impacts from the SCA, EA, and EAWR teleconnections. To our knowledge, these impacts of extratropical teleconnections and Asian monsoon on summer Mediterranean evaporation variability are revealed for the first time, and the obtained detailed

picture of their evolution provides a new contribution to the Mediterranean evaporation literature.

We further investigated the relative roles of atmospheric dynamics (via near surface wind speed) and thermodynamics (through changes in vertical moisture gradient) in the association between teleconnections and Mediterranean evaporation during summer. It is shown, in particular, that the link with the Asian monsoon is mostly through thermodynamics. In contrast, the major player in the SNAO link to Mediterranean evaporation in June is atmospheric dynamics. We also found a dominant role of atmospheric thermodynamics in the relation with SCA and EA in August, and link to EAWR in September. Overall, these results imply an increasing (decreasing) role of atmospheric thermodynamics (dynamics) in evaporation variability from the beginning towards the end of the summer season.

A multiple regression analysis was also conducted between the different teleconnection indices and the leading two Mediterranean evaporation PCs of the summer months to highlight the role of the timescale responsible for the observed Mediterranean evaporation-teleconnection link. The overall outcome of this analysis is the impact of the Asian summer monsoon on Mediterranean evaporation on interannual timescales, especially in late summer because of the varying monsoon onset date, and the effect of the SNAO, which takes place in most summer months on both interannual and decadal timescales. The relationship with the SNAO is not uniform across months, e.g., it is weaker in July. This is not surprising as, for example, the SNAO is weaker and northward shifted, compared to its winter analogue. This partly agrees with results of correlation analysis. It should be stressed, however, that both analyses have their advantages and limitations. In particular, correlation does not take into account the time scale, but is done globally, whereas regression takes into account timescale, but is done only on particular PCs. The sample size is also quite small, which does not allow high significance. This also has an effect on the variance of the EOFs and their degeneracy and hence their separation.

The present study investigated the structure and mechanisms of the summertime Mediterranean evaporation variability. We revealed the major drivers of evaporation variability and demonstrated that their impact is highly variable both in space and time. Significant changes of the relative roles of atmospheric dynamics and thermodynamics in teleconnection impacts on Mediterranean evaporation have been also revealed. This indeed provides deeper insight into the mechanisms driving variability of Mediterranean evaporation. It is expected that new studies based on high resolution data supported by climate model experiments, allowing for reasonably large sample sizes, would provide more accurate assessment of the Mediterranean evaporation variability at different time scales and its possible changes under climate change scenarios.

Declarations

References

Allan RP, Zveryaev II (2011) Variability in the summer season hydrological cycle over the Atlantic-Europe region 1979-2007. Int J Climatol 31:337–348

Barnston AG, Livezey RE (1987) Classification, seasonality and persistence of low-frequency atmospheric circulation patterns. Mon Weather Rev 115:1083–1126

Bendat JS, Piersol AG (1966) Measurement and analysis of random data. J. Wiley & Sons, New York, 390 pp

Borghini M, Bryden H, Schroeder K, Sparnocchia S, Vetrano A (2014) The Mediterranean is becoming saltier. Ocean Sci 10:693–700

Cherchi A, coauthors (2014) South Asian summer monsoon and the Eastern Mediterranean climate: the monsoon-desert mechanism in CMIP5 simulations. J Climate 27:6877–6903

Chronis T, Raitsos DE, Kassis D (2011) The summer North Atlantic oscillation influence on the Eastern Mediterranean. J Clim 24:5584–5596

Enfield DB, Mestas-Nuñez AM, Trimble PJ (2001) The Atlantic multidecadal oscillation and its relation to rainy autumn and river flows in the continental US. Geophys Res Lett 28:2077–2080

Fontaine B, Monerie PA, Gaetani M, Roucou P (2011) Climate adjustments over the African-Indian monsoon regions accompanying Mediterranean Sea thermal variability. J Geophys Res 116:D23122

Hannachi A (2021) Pattern identification and data mining in weather and climate. Springer-Verlag, Berlin, p 416 In press

Hannachi A, Jolliffe IT, Stephenson DB (2007) Empirical orthogonal functions and related techniques in atmospheric science: A review. Int J Climatol 27:1119–1152

Hoskins BJ, Ambrizzi T (1993) Rossby wave propagation on a realistic longitudinally varying flow. J Atmos Sci 50:1661–1671

Kostopuolou E, Jones PD (2007) Comprehensive analysis of the climate variability in the eastern Mediterranean. Part I: map-pattern classification. Int J Climatol 27:1189–1214

Lionello P (2012) The climate of the Mediterranean region: from the past to the future. (P Lionello ed.) 1st Edition. Elsevier, 502 pp

Mariotti A (2010) Recent changes in the Mediterranean water cycle: a pathway toward long-term regional hydroclimatic change? J Clim 23(1513):1525

Mariotti A, Struglia MV, Zeng N et al (2002) The hydrological cycle in the Mediterranean region and implications for the water budget of the Mediterranean Sea. J Clim 15(1674):1690

Mariotti A, Zeng N, Yoon J-H, Artale V, Navarra A, Alpert P, Li LZX (2008) Mediterranean water cycle changes: transition to drier 21st century conditions in observations and CMIP3 simulations. Environ Res Lett 3. https://doi.org/10.1088/1748-9326/3/4/044001

North GR, Bell TL, Calahan RF (1982) Sampling errors in the estimation of empirical orthogonal functions. Mon Weather Rev 110:699–706

O'Reilly CH, coauthors (2017) The dynamical influence of the Atlantic Multidecadal Oscillation on continental climate. J. Climate 30:7213–7230

Papadopoulos VP, coauthors (2012) Influence of atmospheric circulation on turbulent air-sea heat fluxes over the Mediterranean Sea during winter. J Geophys Res 117:C03044. https://doi.org/10.1029/2011JC007455

Parthasarathy B, Munot AA, Kothawale DR (1995) All India monthly and seasonal rainfall series: 1871-1993. Theor Appl Climatol 49:217–224

Pradhan M, Rao AS, Srivastava A, Dakate A, Salunke K, Shameera KS (2017) Prediction of Indian summer monsoon onset variability: A season in advance. Sci Rep 7:14229

Raicich F, Pinardi N, Navarra A (2003) Teleconnections between Indian monsoon and Sahel rainfall and the Mediterranean. Int J Climatol 23:173–186

Rizou D, Flocas HA, Athanasiadis P, Bartzokas A (2015) Relationship between the Indian summer monsoon and the large-scale circulation variability over the Mediterranean. Atmos Res 152:159–169

Rodwell MJ, Hoskins BJ (1996) Monsoons and the dynamics of deserts. Q J Roy Meteorol Soc 122:1385–1404

Sandoval-Gil JM, Marin-Guirao L, Ruiz JM (2012) The effect of salinity increase in the photosynthesis, growth and survival of the Mediterranean seagrass *Cymodocea nodosa*. Estuar Coast Shelf Sci 115:260–271

Simpson IR, coauthors (2015) Mediterranean summer climate and the importance of Middle East topography. *J. Climate* 28:1977–1996

Soman MK, Kumar K (1993) Space-time evolution of meteorological features associated with the onset of the Indian summer monsoon. Mon Weather Rev 121:1177–1194

von Storch H, Navarra A (1995) Analysis of Climate Variability. Springer-Verlag, New-York, 334 pp

Webster PJ, Yang S (1992) Monsoon and ENSO: Selectively interactive systems. Q J Ro Meteorol Soc 118:877–926

Wilks DS (1995) Statistical Methods in the Atmospheric Sciences. 2nd Edition, Academic Press, 627 pp

Yu L (2007) Global variations in oceanic evaporation (1958–2005): The Role of the Changing Wind Speed. *J. Climate* 20(21):5376–5390

Yu L, Weller RA (2007) Objectively analyzed air-sea heat fluxes for the global ice-free oceans (1981-2005). Bull Am Meteorol Soc 88:527–539

Zveryaev II, Hannachi AA (2012) Interannual variability of Mediterranean evaporation and its relation to regional climate. Clim Dyn 38:495–512. https://doi.org/10.1007/s00382-011-1218-7

Zveryaev II, Hannachi AA (2017) Interdecadal changes in the links between Mediterranean evaporation and regional atmospheric dynamics during extended cold season. Int J Climatol 37:1322–1340. https://doi.org/10.1002/joc.4779